

Statistics and kinetics of single-molecule electron transfer dynamics in complex environments: A simulation model study

Luciana C. Paula, Jin Wang, and Vitor B. Leite

Citation: *J. Chem. Phys.* **129**, 224504 (2008); doi: 10.1063/1.3036421

View online: <http://dx.doi.org/10.1063/1.3036421>

View Table of Contents: <http://jcp.aip.org/resource/1/JCPSA6/v129/i22>

Published by the **AIP Publishing LLC**.

Additional information on *J. Chem. Phys.*

Journal Homepage: <http://jcp.aip.org/>

Journal Information: http://jcp.aip.org/about/about_the_journal

Top downloads: http://jcp.aip.org/features/most_downloaded

Information for Authors: <http://jcp.aip.org/authors>

ADVERTISEMENT



Explore the **Most Cited**
Collection in Applied Physics

AIP
Publishing

Statistics and kinetics of single-molecule electron transfer dynamics in complex environments: A simulation model study

Luciana C. Paula,^{1,2} Jin Wang,^{3,4} and Vitor B. P. Leite^{1,a)}

¹*Departamento de Física, Instituto de Biociências Letras e Ciências Exatas, Universidade Estadual Paulista, São José do Rio Preto, São Paulo 15054-000, Brazil*

²*Departamento de Estudos Básicos e Instrumentais, Universidade Estadual do Sudoeste da Bahia, Itapetinga, Bahia 45700-000, Brazil*

³*Department of Chemistry, Physics and Applied Mathematics, State University of New York at Stony Brook, Stony Brook, New York 11794-3800, USA*

⁴*State Key Laboratory of Electroanalytical Chemistry, Changchun Institute of Applied Chemistry of Chinese Academy of Sciences, Changchun 130022, People's Republic of China*

(Received 2 June 2008; accepted 5 November 2008; published online 9 December 2008)

Dynamics of the environments of complex systems such as biomolecules, polar solvents, and glass plays an important role in controlling electron transfer reactions. The kinetics is determined by the nature of a complex multidimensional landscape. By quantifying the mean and high-order statistics of the first-passage time and the associated ratios, the dynamics in electron transfer reactions controlled by the environments can be revealed. We consider real experimental conditions with finite observation time windows. At high temperatures, exponential kinetics is observed and there are multiple kinetic paths leading to the product state. At and below an intermediate temperature, nonexponential kinetics starts to appear, revealing the nature of the distribution of local traps on the landscape. Discrete kinetic paths emerge. At very low temperatures, nonexponential kinetics continues to be observed. We point out that the size of the observational time window is crucial in revealing the intrinsic nature of the real kinetics. The mean first-passage time is defined as a characteristic time. Only when the observational time window is significantly larger than this characteristic time does one have the opportunity to collect enough statistics to capture rare statistical fluctuations and characterize the kinetics accurately. © 2008 American Institute of Physics. [DOI: 10.1063/1.3036421]

I. INTRODUCTION

Electron transfer (ET) is a ubiquitous reaction that governs many natural and biological processes. Environments have great impacts on the ET dynamics, and it becomes crucial to describe them accurately. In simple solids and liquids, the environments can be mimicked by a set of harmonic oscillators or quadratic local energy wells.¹⁻³ For more complicated environments such as glass, complex viscous liquids, and biomolecules, the environments often display large nonlocal conformational changes, which in general cannot be described simply by means of local harmonic energy wells.

Complex environments, when taking into account their anharmonicity and cooperativity, are best described by a network of orientation spin vectors. Each vector represents, for example, the spins interacting with each other in spin glass systems, the polarizations of polar solvent molecules interacting with each other in solvents, or the polypeptide monomers in protein folding.⁴⁻⁶ In biomolecules, the monomers in the polypeptide chain can take on various orientations, which can also be described by spin vectors. The energies of the whole environment can be changed by flipping the states of the spins in the network. The resulting conformational energies can vary quite significantly between one state of the

environment and another. This pictorial view captures the essential features of the large conformational changes in complex environments. This description has been quantified to study glass,^{7,8} spin glass,⁴ biomolecules,⁹ protein folding,⁵ and complex solvents.⁶ There are quantitative agreements between theory and experiments.⁵

Marcus's theory¹⁻³ of ET describes the influence of solvent to ET reactions by a single collective reaction coordinate, in which the activation barriers are calculated. The rate calculation for nonadiabatic ET reactions in solutions was first addressed by Levich and Dogonadze.¹⁰ Marcus's theory describes the influence of solvent on ET reactions by a single collective reaction coordinate. It divides the nuclear degrees of freedom coupled to the reaction in two groups. "Inner sphere" coordinates are composed of a few intramolecular vibrational modes. The other group is represented by a single "outer sphere" continuous classical collective coordinate, which describes the rearrangement of the remaining degrees of freedom and accounts mostly for the polarization of the solvent. Therefore, a single reaction coordinate characterizes the environmental behavior in the course of the reaction. The free energy profile of this one-dimensional coordinate appears to be smooth. In general, the environmental dynamics occurs on a high-dimensional surface with a large number of energy valleys. The treatment of a reaction coordinate in an explicit way often becomes very difficult due to the large

^{a)}Author to whom correspondence should be addressed. Electronic mail: vbpleite@gmail.com.

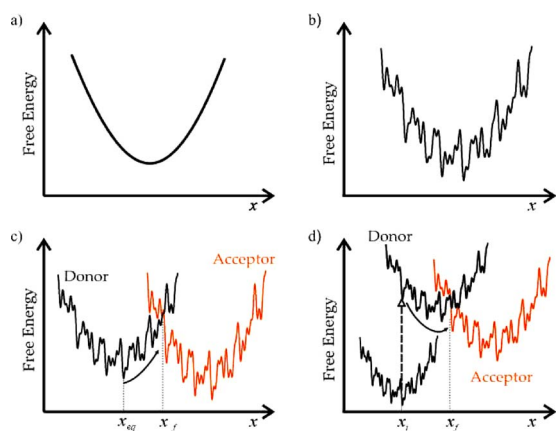


FIG. 1. (Color online) (a) Smooth free energy as a function of reaction coordinate. (b) Pictorial view of rugged free energy as a function of reaction coordinate. Donor and acceptor energy surfaces for nonadiabatic reactions: (c) The system diffuses from equilibrium to an activation polarization. (d) ET occurs after electronic excitation and solvent relaxation.

number of conformational degrees of freedom involved, such as the positions and the orientations of each solvent molecule (solvent coordinates). It is thus important to ask when the single collective coordinate description of Marcus breaks down and the general multidimensional description of the landscape becomes necessary.

This question has been addressed by Onuchic and Wolynes.⁶ They considered a polar solvent (composed of spins) interacting with a charged cavity, representing the donor or acceptor site for ET. A simple discrete analytical model was used to treat each solvent molecule independently. For every temperature, this model has two regions in polarization space. A glassy trappinglike region with multidimensional valleys of the underlying solvent landscape, and another, exhibiting normal diffusive dynamics, in which the one-dimensional effective coordinate picture of Marcus is recovered. Further realistic studies taking care of the outer shells for different layers of solvents have been conducted,¹¹ with trapping transitions found in each corresponding layer. Onuchic and Wolynes⁶ studied the polarization-dependent thermodynamic phase transition for this model, and Leite and co-worker^{12,13} showed that the reactive region has a slow dynamics below the transition temperatures; they argued that this phase transition influences the dynamics of the system. Leite *et al.*¹⁴ further discussed the influences of glassy trapping on kinetics. The ET process can therefore be discussed as motions on, and transitions between, multidimensional potential energy surfaces. These surfaces represent the potential energy of the system (electronic donor and acceptor states) as a function of a reaction coordinate, as shown in Fig. 1. For a smooth landscape a single coordinate description is appropriate, and in a rugged landscape a multidimensional description is necessary.

In the present study, we consider a rather general polar reaction medium, which allows for not only small amplitude response around a stable state, but also incorporates the possibility of a hierarchy, or landscape, of metastable states. However, the model traced back to the Onuchic and Wolynes (OW)⁶ model of a frustrated dipole system is augmented by the possibility that the landscape may not be spatially homo-

geneous. This is a real possibility in slow solvents (polymeric, glassy, etc.), or when clathrate structures are present, or in biological systems with many conformations. The presence of such a structured bath leads to a variety of particle transfer reactions with complex kinetics. Such kinetics are quite common, which has become especially obvious with the advent of single-molecule spectroscopy. But even if the kinetics are exponential, the temperature dependence of the transfer rate often does not match the well behaved Marcus theory. Clearly, assuming a temperature-dependent reorganization energy, etc., to fit the data, it is not so revealing. One needs a new picture. Our way of studying the statistical nature of the underlying solvent landscape will naturally lead to a new picture of the temperature behavior of the kinetic rates.

With quantitative description of the environments using energy landscape theory, we study the kinetics of ET reactions under the influence of environmental fluctuations. The characterization of environmental fluctuations and the underlying energy landscape can be revealed in single-molecule experiments, such as that carried out by Kou and Xie.¹⁵ In bulk measurement, the only observable information about the system consists of the average values. For single molecules, complete dynamic information, such as high-order statistical fluctuations and distribution of the observables, can be obtained. In particular, the information on kinetics, such as first-passage time (FPT), its higher-order moments, and its associated distribution, can be studied,^{16–21} which was also the focus of our model.

We modeled the environmental conformational fluctuations of biomolecule dynamics with a system of orientation vectors (or spins) interacting with each other. We investigated the influence on ET reaction kinetics as a function of temperature. We found that the kinetics experiences a transition from the high-temperature self-averaging exponential behavior to low-temperature non-self-averaging nonexponential behavior. In this case, nonexponential kinetics implies non-Poisson statistics. This leads to intermittency phenomena where slow-decaying (long) distribution tails develop and high-order moments become important.^{16–21} High-order statistical information can thus provide important clues in determining dynamics. In other words, rare events (low probability events) can be crucial. In bulk, these fluctuations are suppressed by the large number of molecules and cannot be seen. In single molecules, in principle, one can explicitly measure these fluctuations and the corresponding statistics. At even lower temperature, we found that the kinetics continues to be nonexponential.

II. MODEL AND SIMULATIONS

A. Model

The polar environment can be modeled as a single shell of solvent molecules with simple rotational dynamics around a charge cavity.⁶ The molecules are represented by dipoles pointing only in two directions, as Ising spins, as shown in Fig. 2. Once the dipoles are (randomly) set in the cavity, they

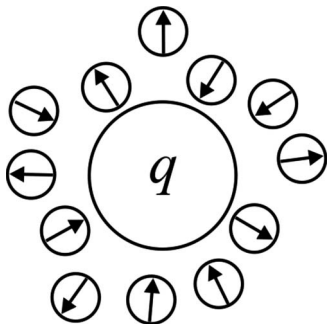


FIG. 2. Single-shell OW model for solvent dipoles around a cavity with charge q .

are fixed in their positions, and they are allowed only to rotate, taking one of two possible orientations, within or outside the cavity.

The solvation energy is given by

$$E_{\text{solv}} = - \sum_{i=1}^N \xi_i(q) \sigma_z(i) + \sum_{\langle ij \rangle} J_{ij} [\sigma_z(i), \sigma_z(j), \mathbf{r}_i, \mathbf{r}_j], \quad (1)$$

where the first term is the dipole-charge interaction and the second term the dipole-dipole one. q is an index associated with the cavity charge.

Due to the random nature of the heterogeneous interactions, the solvent model follows the random energy model²² approximation to evaluate the solvent energies, which assumes the energies are given by Gaussianly distributed random variables. For each set of dipole orientations $\{\sigma_z(i)\}$, a random energy is assigned. Since we have N dipoles, the total number of states of the system is 2^N .

The total polarization per dipole x is used as the reaction coordinate for the solvent, and it is defined by

$$x = (n_+ - n_-)/N, \quad (2)$$

where N is the total number of dipoles, and n_+ (n_-) is the number of dipoles oriented within (outside) the charge cavity. The number of oriented dipoles follows the constraint

$$n_+ + n_- = N. \quad (3)$$

The free energy depending on total polarization is used as the effective potential. Typical energy surfaces for different electronic states in ET reactions are shown in Fig. 1. The standard deviation of the solvation energy ΔE is assumed to be independent of x and scales with $N^{1/2}$. $\Delta E = N^{1/2} \Delta \varepsilon$, where $\Delta \varepsilon$ sets the energy scale in our simulation. The average solvation energy is

$$\bar{E}(x) = \bar{J}(x - x_{\text{eq}})^2/N, \quad (4)$$

where x_{eq} is the equilibrium polarization of the cavity and \bar{J} is a constant associated with dipole-charge interaction.^{12,13} The energy probability distribution $g(x, E)$ at polarization x is

$$g(x, E) = \frac{1}{\sqrt{2\pi\Delta E}} \exp\left[-\frac{(E - \bar{E}(x))^2}{2\Delta E^2}\right], \quad (5)$$

which leads to an average number of states with polarization x and energy between E and $E+dE$ given by

$$\langle n(x, E) \rangle = \Omega(Nx) g(x, E) dE, \quad (6)$$

where

$$\Omega(Nx) = \frac{N!}{n_+! n_-!} = \frac{N!}{[N(1-x)/2]! [N(1+x)/2]!}$$

is the total number of states with polarization x . For $\langle n(x, E) \rangle \gg 1$, one can approximate $\langle \log n(x, E) \rangle$ by $\log \langle n(x, E) \rangle$, and the entropy becomes

$$S(x, E) \approx \log \langle n(x, E) \rangle \approx \log \Omega(Nx) - \frac{(E - \bar{E}(x))^2}{2\Delta E^2}. \quad (7)$$

At the critical energy

$$E_c(x) = \bar{E}(x) - \Delta E (2 \log \Omega(Nx))^{1/2}, \quad (8)$$

the entropy vanishes, and Eq. (7) approximation is not valid. The system becomes frozen into a small number of states with low energies. At the thermodynamic limit for $E < E_c(x)$, instead of Eq. (7), $S(x, E) = 0$. Using the thermodynamic Maxwell relationship

$$\partial S / \partial E = 1/T, \quad (9)$$

where T is the temperature, when calculated at E_c , it gives the (glassy) transition temperatures.

B. Transition temperatures

By exploring the underlying free energy landscape, the overall phases and behaviors of the system can be studied. In general, a high-temperature smooth phase and a low-temperature trapping phase are found.^{6,12,13} In this work we explored two kinds of phase transition temperatures.¹²

(a) *Global phase transition* is associated with the total number of states (2^N). It is characterized by

$$S^g(E) = \log[2^N g(E)] = 0, \quad (10)$$

where $S^g(E)$ is the total entropy, and $g(E)$ is the energy probability distribution. Using Eqs. (7) and (9),

$$\beta_c^g = \frac{1}{T_c^g} = \frac{[2N \log 2]^{1/2}}{\Delta E} = \frac{(2 \log 2)^{1/2}}{\Delta \varepsilon}, \quad (11)$$

the transition temperature is given by $\beta_g = T_g^{-1} = \sqrt{2 \ln(2)} \approx 1.18$, in units of $\Delta \varepsilon / k_B (=1)$. This corresponds to the thermodynamic phase transition of the system. At or below this temperature, the system is thermodynamically trapped. Ergodicity breaks down for the system and non-self-averaging behavior can be seen. A system can have very different behaviors at different regions of the phase space.

(b) *Local phase transition* is a kinetic transition that occurs when the system starts to become trapped into local minima. Below this temperature, escapes from local minima go preferentially through neighboring states with the smallest barrier instead of overcoming a typical barrier,

$$\beta_{\text{loc}} = T_{\text{loc}}^{-1} = [2 \ln(M)/M]^{1/2}, \quad (12)$$

where M is the number of states kinetically connected to a given state.

In this work, we explored the kinetics by specifying the kinetic rules allowing only a single dipole flip per elementary move ($M=N$), with move acceptance based on a Monte Carlo Metropolis procedure, such that when $E_{\text{now}} > E_{\text{next}}$, the move is accepted with probability 1; and when $E_{\text{now}} < E_{\text{next}}$, the move is accepted with probability $\exp[-\beta(E_{\text{next}} - E_{\text{now}})]$, where $\beta = 1/kT$. It is worth mentioning that Monte Carlo moves do not in general correspond to the real kinetic moves, but the total of Monte Carlo steps gives an estimate (proportional to) of the total kinetic times. In our simulations $N=20$, so $\beta_{\text{loc}}=0.54$.

The OW model also predicts that, for every polarization x , there is a critical temperature, the *polarization-dependent phase transition* ($T_c(x)$), given by

$$\beta_c(x) = \frac{1}{T_c(x)} = \frac{\partial S}{\partial E} \Big|_{E=E_c(x)} = \frac{[2S^*(Nx)]^{1/2}}{\Delta E}, \quad (13)$$

where $S^*(Nx) = \log \Omega(Nx)$ is the configuration entropy.

At a particular temperature T , such that $T = T_c(x_0)$, for $|x| < |x_0|$ the system has a behavior like the standard Born–Marcus model. As it reaches x_0 , the dynamics becomes glassy. When one compares the values for T_{loc} , $T_c(x)$, and T_g , it can be observed that they occur in the following order:

$$T_{\text{loc}} > T_c(x) > T_g, \quad (14)$$

such that the polarization-dependent phase transition is manifested as a subtle kinetic behavior.

C. Kinetics and high-order statistical fluctuations

In the Marcus description in the nonadiabatic regime, ET reactions are assumed to take place when the system reaches the reactive region (x_f in Fig. 1). The dynamics of this system can be studied by the FPT of ET events, which is the time the system takes to diffuse from an initial total polarization x_i to another final polarization x_f , where the ET takes place. Its mean is denoted by τ (*mean* FPT). A way of measuring the significance of the high-order statistics of the fluctuations—the intermittency—is to observe the ratio between the average of the n th order moment and the n th power of the first moment,^{14,21}

$$R_n = \frac{\langle t^n \rangle}{\langle t \rangle^n}, \quad (15)$$

where $\langle t \rangle = \tau$.

It must be stressed that transition state theory only accounts for the exponential part of the kinetics regarding the barrier height. Many barrier recrossings occur in the nonadiabatic case, which are important and contribute to the kinetics through the prefactor or transmission coefficient, and cannot be ignored.²³ Our FPT kinetics analysis emphasizes the exponential part of the barrier regarding the height. Since our FPT analysis is more connected with the barrier height, for nonadiabatic studies where recrossings often occur, full

kinetics information, such as survival probability, is needed. We will explore this in detail in a future study.

At high temperature, the system is well behaved, it is expected that the times of occurrence obey an exponential behavior with a single constant rate of reaction, $k = \tau^{-1}$, and the survival probability of events follows Poisson exponential kinetics¹⁷

$$p(t) = ke^{-kt}. \quad (16)$$

The n th order moment can be computed by

$$\langle t^n \rangle = \int_0^\infty t^n \frac{dp(t)}{dt} dt = \frac{n!}{k^n}; \quad (17)$$

thus, the ratio $R_n = n!$ characterizes a system with exponential dynamics. The FPT distribution of the reaction coordinate (solvent) events as a function of logarithm of time is given by

$$f(y) = k \exp(y - e^y), \quad (18)$$

where $y = \ln(t)$.

Below the transition temperatures, fluctuations in the FPT become significant, $R_n/n! > 1$, and $f(y)$ deviates from the above expression. The increase in this ratio indicates that statistics have deviated from Poisson statistics. It implies that high-order moments are becoming more and more important. Slow-decaying (long) tails in the distribution start to develop. Intermittency, where rare events play crucial roles in dynamics, is observed.

D. Simulations

The kinetic rules of our simulations allow only a single dipole flip per elementary move, with move acceptance being based on a Monte Carlo procedure.^{12–14} A simulation with 20 dipoles was carried out with $\Delta E = 20^{1/2} \Delta \epsilon$ ($\Delta \epsilon/k_B = 1$) and $\bar{E}(x) = 0$. In the simulations, the energy for the system is fixed according to the random energy model^{6,22} for each of the 2^N states. Different runs correspond to variations in the states of the dipole orientations (+1 or –1). We investigated two different types of reactions controlled by the environments. The first of these were the thermally activated uphill reactions, illustrated in Fig. 1(c). After thermal equilibration the system starts at $x_i = x_{\text{eq}} = 0$ and diffuses to $x_f = 0.5$. At temperatures around T_{loc} , local minima will be populated. As the temperature is lowered, T_{loc} will be the first transition temperature occurring in the system. All FPTs were computed with the same energy assignment, but under different initial conditions.

The second type of reaction schemes simulated here corresponds to a downhill relaxation process followed by ET reaction. It mimics experiments where the molecule in the cavity undergoes a dipole shift upon electronic excitation, which changes the equilibrium polarization, as shown in Fig. 1(d). The system relaxes from high-energy states and does not get easily trapped at local minima. The system was simulated initially excited leaving the initial polarization $x = -0.5$ until the final polarization $x = 0.1$. As in the activation case, the simulation has a limited number of Monte Carlo steps to reach the final polarization. This is an atypical case

in the sense that the system diffusing randomly needs only a few steps to reach the final polarization due to the inherent downhill process.

III. RESULTS

Some of the difficulties in studying real glassy systems are associated with the experiments' time duration as well as the signal/noise ratio, particularly on investigation of glassy kinetics below glass transition temperatures. When one probes intermittency, where rare events become important, some obvious questions arise: How many rare events are needed to characterize the intermittency? How do we compare these rare events with the average ones? In other words, from the experimental perspective, how long must the experimental time duration be to appropriately probe the intermittency. We address these questions as well as the characterization of such transitions.

For two different types of reactions controlled by solvent, we analyzed phase transitions by means of high-order statistical fluctuations in kinetics through moment ratios. Moreover sensibility of moment ratios R_n is investigated using an observation time window. In Sec. III A thermally activated reactions are studied. In Sec. III B we discuss the relaxation process.

A. Thermally activated reactions

As in Fig. 1(c), simulations were performed for the activation process, limiting the time allowed for the system to reach x_f . We looked at time window J from 10^4 to 10^9 . The results of the high-order statistical fluctuations in kinetics through the ratio of n th order moment of FPT and average FPT raised to the n th power, $R_n/n!$, are shown in Fig. 3. One can see that, with exception of $J=10^4$, there is a divergence of $R_n/n!$ around the local transition temperature, $\beta \approx 0.5$. This means the kinetics becomes divergent and non-self-averaging. Average kinetics are insufficient to characterize the system. Intermittency occurs where rare events can become important,^{14,16,17,20,21} reflecting the fact that the underlying energy landscape has become rough. As J increases, $R_n/n!$ becomes larger at lower T . The existence of a maximum for $R_n/n!(T)$ is due to the finite observation time, which varies with J and is expected to vary from one system to another. The larger the observational time window, the more statistical information on kinetics can be collected, the more chances of capturing the rare events of large fluctuations represented by the high values of the moment ratio, and the more accurate can the description of the kinetics be.

The relevant question is as follows: What is the transition temperature at which $R_n/n!$ starts to diverge from 1? And also what is the criterion for defining and selecting the observation time window J ? Of course it does not make sense to look for an absolute value for observation time window J in Monte Carlo step units, but a general problem is to find a procedure for estimating appropriate J compared with the average time of events (averaged FPT), τ . Since τ does not vary significantly with the occurrence of rare events, we

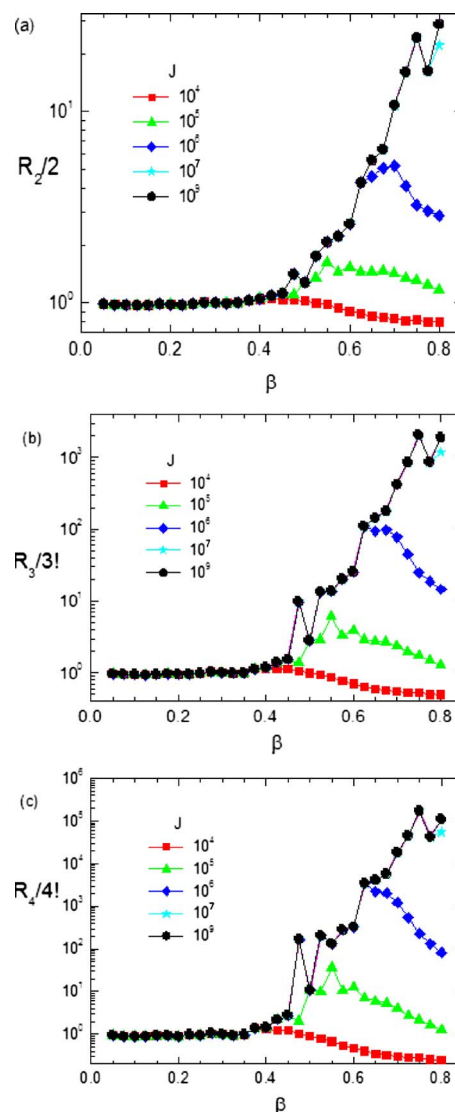


FIG. 3. (Color online) $R_n/n!$ as a function of inverse temperature for different observation windows J in the thermally activated process simulation (from equilibrium to activated state).

can sort all time occurrences of simulation events in increasing order. We observe how τ reaches its actual value at ideal sampling.

Figure 4(a) shows how τ reaches its asymptotic value as a function of J in terms of Monte Carlo time steps for various temperatures β . As we can see, when the observation time window is significantly smaller than the intrinsic average kinetic time, the observational average time is strongly correlated with the size of the observational time window and therefore not a reliable estimate of the real kinetics. On the other hand, when the observational time window is significantly larger than the intrinsic average kinetic time, the observational averaged time reaches a plateau value close to the real averaged kinetics. The criterion for this convergence can vary with temperatures. The lower the temperatures (the larger β), the longer the observational time window has to be in order to capture the intrinsic slow kinetics. In our case we considered the estimated value of the characteristic minimum time for the observational window at which the tangent in

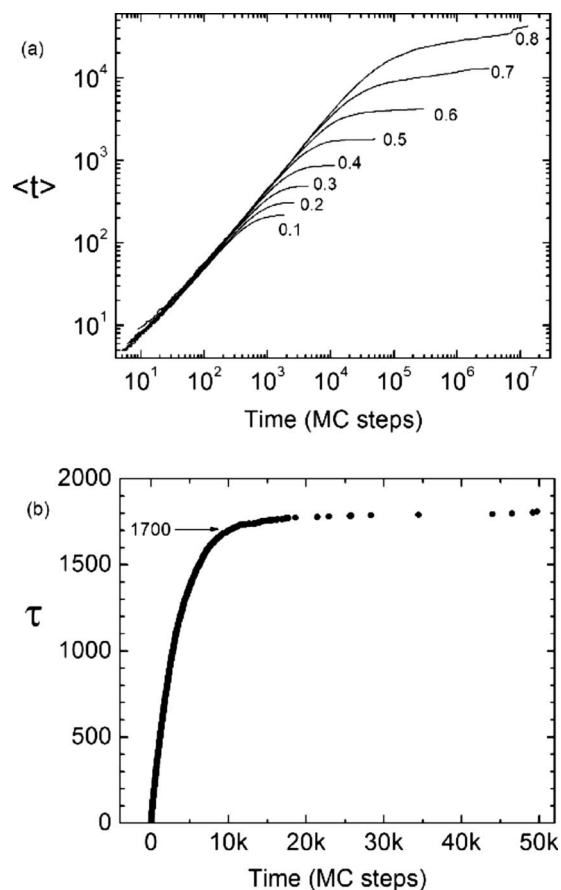


FIG. 4. (a) Asymptotic value of the mean FPT for several inverse temperatures (β) as a function of observation window J in units of Monte Carlo steps for thermally activated process simulation. (b) Graphic representation of characteristic estimation of asymptotic mean first passage, τ_{est} , for $\beta=0.5$.

the curve τ versus J has an inclination of 10° , that is, the average time τ reaching an asymptotic value as in Fig. 4(b).

Next we calculate the high-order statistical fluctuations in kinetics $R_n/n!$ to probe the topography of the underlying landscapes for various values of observational time window J , in multiples of characteristic time τ , shown in Fig. 5 ($10 \times \tau_{\text{est}}$, $30 \times \tau_{\text{est}}$, and $100 \times \tau_{\text{est}}$). At high temperatures, the underlying landscape becomes smooth, and it is quite easy to pass from one place to another. Multiple kinetic routes are available. On the other hand, when the temperature drops, the underlying landscape becomes rougher. The kinetics becomes slower. There are, in general, only a discrete number of kinetic routes possible. We can start to see the non-self-averaging effects through the higher fluctuations in kinetics from moment ratios. We see that if we choose an observational time window size significantly larger than the characteristic average time τ , then we will have better chances of seeing the high values of the moment ratios as shown in Fig. 5 and therefore of capturing the rare events of high statistical fluctuations. Using the averaged FPT, as a characteristic time for gauging the observation window, it seems to provide an efficient way for guiding the modeling and simulations to capture the essence of the complex system dynamics.

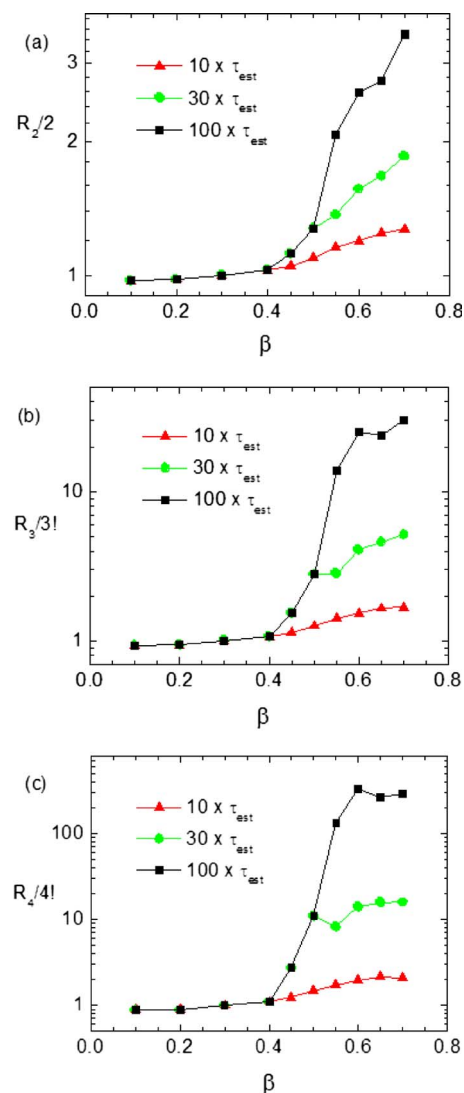


FIG. 5. (Color online) $R_n/n!$ for $n=2, 3$, and 4 as a function of inverse temperature for thermally activated process simulation, with different window sizes in units of τ_{est} .

B. Relaxation process

As mentioned in Sec. II D, the relaxation is a relatively fast downhill process. In this case, with a small number of flipping dipole orientations to reach the final state, the statistics can become distorted. This fact is evidenced in Fig. 6, which shows the kinetics in terms of the survival probability $P(t)$ versus time at several different temperatures. We can see that, even at high temperatures, the relaxation process does not exhibit an exact exponential decay. The lower the temperature, the farther away the kinetics is from the exponential and becomes more nonexponential (solid curves represent exponential kinetics). This reflects the fact that the underlying landscape becomes rougher at lower temperature.

The simulations were performed under ideal conditions, i.e., all events were computed. In real experimental situations there is noise and one can only work with a finite observation time window, so the rare events that are responsible for the increase in high-order statistical fluctuations characterized by the moment ratio $R_n/n!$ may not be detected. To simulate real experimental conditions, we need to vary the observa-

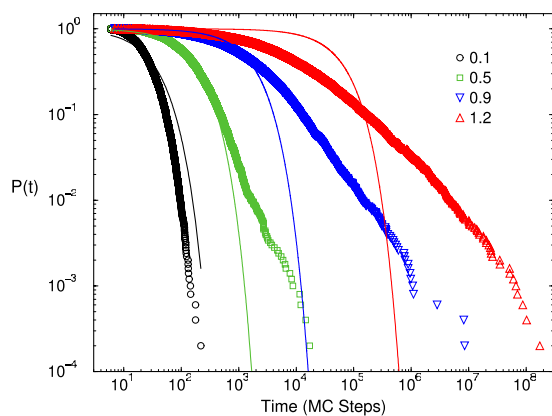


FIG. 6. (Color online) Survival probability $P(t)$ as a function of time (in Monte Carlo steps) for different inverse temperatures in the relaxation process simulation. The continuous line is their fit with a exponential decay function. In none of these cases, the fittings correspond to a real exponential decay.

tional window size corresponding to the relaxation process. This is accomplished by varying the allowed Monte Carlo steps. The events that occurred at times outside the window size will be neglected. Figure 7 shows statistical fluctuations in kinetics quantified by the moment ratio $R_n/n!$ for different windows scaled as multiples of the mean FPT. We can see once again that, at high temperatures, the kinetics is self-averaging without much statistical fluctuation, reflecting the underlying smooth landscape. On the other hand, as the temperatures drop, the statistical fluctuations become more and more significant, as shown in Fig. 7 by the smooth increase in the moment ratio with respect to temperature decrease (or increase of $\beta=1/kT$). This reflects the fact that the underlying landscape becomes more and more rough and kinetics become more and more non-self-averaging. The rare events characterized by the high values of the moment ratio can become more important in describing the kinetics accurately. If the window size is too small, then we observe a drop in the fluctuations. This is due to the fact that there is not enough observational time to see the rare large statistical fluctuations. This can be very misleading¹⁴ since observation does not reflect the real intrinsic kinetics of the system. When the size of the observational time window increases, we observe less and less of the drop in the statistical fluctuations with respect to the temperature drop. This reflects the fact that, as the observational times become longer, one has a better chance of catching the large intrinsic statistical fluctuations in kinetics. There is no drop in the statistical fluctuations at lower temperatures if we have a long enough observational time window. Therefore, the relaxation process must be analyzed in a more careful way, using, for example, a model involving a larger number of dipoles.

At very low temperatures, we need a longer observational time window in order to have enough statistics for characterizing the behavior of the system. With only a short observational time window, we observe that the moment ratio diminishes as temperatures drop, which could imply fewer fluctuations and more single exponential behavior for an underlying Poisson process.¹⁴ With a sufficient observational time window, we see that, even at very low tempera-

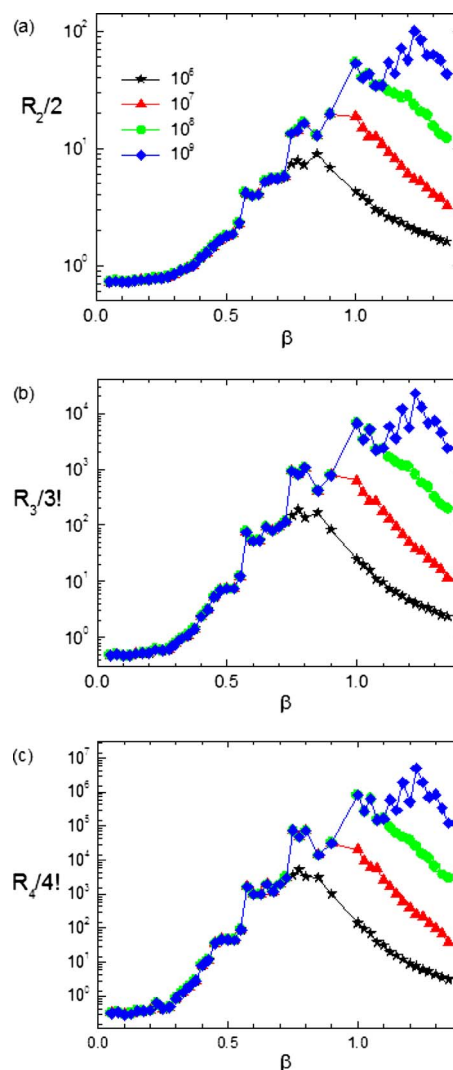


FIG. 7. (Color online) $R_n/n!$ as a function of inverse temperature for different observation windows J for the relaxation process simulation.

tures, the moment ratio remains high, implying the nonexponential non-Poisson behavior reflecting the rough underlying landscapes.

IV. CONCLUSION AND DISCUSSIONS

In this paper, we have investigated the kinetics and statistics of ET in general solvents mimicking complex environments such as glass, viscous liquids, or biological molecules. We have found that two characteristic temperatures control the nature of the kinetics. For relaxation processes, changes in kinetic regimes are associated with the global trapping temperature. For the thermally activated processes, changes in kinetic regimes are associated with the local trapping temperature. Both parameters act as markers where, at temperatures well above them, the kinetic process is single exponential; at temperatures around them, the kinetic process becomes nonexponential; while, at temperatures well below them, the kinetic process continues to be nonexponential.

Similar kinetic behavior is observed in biomolecular folding.²⁴ We believe this exponential to nonexponential transition in temperature to be universal in complex systems. The rationale behind this is the following: At high tempera-

tures, there are kinetically multiple routes to the final states, since high temperatures imply high kinetic energy, which means that kinetic energy dominates potential energy, so the kinetics “senses” only the average barrier and each kinetic path is more or less equivalent to the others. This explains why high-temperature kinetics is single exponential.

On the other hand, when the temperature is near the characteristic temperature T_{loc} , there are limited conformational spaces to explore and the kinetic process becomes non-self-averaging. In other words, each path becomes more and more distinct from the others. Since each path senses a different barrier, there is a distribution of kinetic rates rather than a single rate, and the kinetics thus becomes nonexponential. When the states are nearly trapped or frozen, the original Gaussian normal density of states can be linearized and expand around the mean in the exponential, thus becoming exponential. This will lead typically to the power law distribution of FPT or the kinetic rate. This kind of kinetic phenomenon has been seen in single-molecule ET experiments probing the underlying landscape of biomolecules (solvents) in Kou and Xie’s experiments.¹⁵

In Kou and Xie’s experiments, the ET kinetics in a single protein molecule is measured through the fluorescence lifetime. The fluorescence lifetime is correlated with the inherent ET rate. By measuring the time trace or distribution of the fluorescence lifetime, Xie and co-workers can infer the fluctuations in single-molecule transfer kinetics. Furthermore, by using the ET rate formula and the dependence on the distance between the donor and acceptor, they were able to explore the underlying conformational fluctuations of the protein through ET. The correlation function of the lifetime shows highly nonexponential behavior (fitted well with stretched exponential) and the distribution in distance reflecting the underlying protein motion is broadly distributed (power law).

In this study, we have explored both the average and high-order fluctuations of electron kinetics. It is clear that fluctuations in kinetics through high-order moments are significant and non-Poisson. The resulting statistics in kinetics is nonexponential. Furthermore, when we studied the probability distribution of kinetics times, we found that, as temperature drops, the log-log plot is almost linear. This indicates that the distribution of kinetics is broad and approaches power law. These results support Kou and Xie’s single-molecule ET experiment. We can also predict the trend of the power law coefficient on temperature from our study. This shows how temperature modulates the underlying conformational landscape of proteins. We propose a future single-molecule ET experiment to test the temperature dependence of statistics on kinetics.

We have pointed out that the size of the observational time window is crucial in revealing the intrinsic natures of the real kinetics. We define a characteristic time as the mean FPT. Only when the observational time window is significantly larger than the defined characteristic time does one have the chance to collect enough statistics to capture rare statistical fluctuations and characterize the kinetics accurately. This is an important message for both single-molecule spectroscopist and molecular modelers.

In the well-known joke concerning the drunk looking for his keys in light beneath a lamppost, it will be recalled that a passerby enquired why he was looking in that particular place, if he did not know where he had lost his keys. The drunk replied that he was looking there because that was where the light was best. We may understand from that joke that one should search for answers where one has the best chance of finding them. By analogy, our results suggest that, if one hopes to encounter the true kinetics, one should not go too close to the edge of the experimentally available dynamical range.

ACKNOWLEDGMENTS

We thank J. N. Onuchic for helpful discussions. We also thank the two referees for very insightful comments. L.C.P. and V.B.P.L. were supported by Fundação de Amparo à Pesquisa do Estado de São Paulo (FAPESP), Brazil. V.B.P.L. is also supported by CNPq, Brazil. J.W. is supported by National Science Foundation Career Award, American Chemical Society Petroleum Research Fund.

- ¹R. A. Marcus, *J. Chem. Phys.* **24**, 966 (1956).
- ²P. J. Steinbach, A. Ansari, J. Berendzen, D. Braunstein, K. Chu, B. R. Cowen, D. Ehrenstein, H. Frauenfelder, J. B. Johnson, D. C. Lamb, S. Luck, J. R. Mourant, G. U. Nienhaus, P. Ormos, R. Philipp, A. H. Xie, and R. D. Young, *Biochemistry* **30**, 3988 (1991); N. Agmon and J. J. Hopfield, *J. Chem. Phys.* **79**, 2042 (1983); I. Rips and J. Jortner, *ibid.* **87**, 2090 (1987); H. Sumi and R. Marcus, *ibid.* **84**, 4272 (1986); W. Nadler and R. Marcus, *ibid.* **86**, 3906 (1987).
- ³M. D. Newton and H. L. Friedman, *J. Chem. Phys.* **88**, 4460 (1988); **89**, 3400 (1988).
- ⁴M. Mezard, G. Parisi, and M. A. Virasoro, *Spin Glass and Beyond* (World Scientific, Singapore, 1987).
- ⁵J. D. Bryngelson, J. N. Onuchic, N. D. Socci, and P. G. Wolynes, *Proteins: Struct., Funct., Genet.* **21**, 167 (1995).
- ⁶J. N. Onuchic and P. G. Wolynes, *J. Chem. Phys.* **98**, 2218 (2003).
- ⁷F. H. Stillinger and T. Weber, *Science* **225**, 983 (1984).
- ⁸V. Lubchenko and P. G. Wolynes, *Annu. Rev. Phys. Chem.* **58**, 235 (2006).
- ⁹H. Frauenfelder, F. Parak, and R. D. Young, *Annu. Rev. Biophys. Biochem. Chem.* **17**, 451 (1988); H. Frauenfelder, S. G. Sligar, and P. G. Wolynes, *Science* **254**, 1598 (1991).
- ¹⁰V. G. Levich and R. R. Dogonadze, *Dokl. Akad. Nauk SSSR* **124**, 123 (1959).
- ¹¹Y. Tanimura, V. B. P. Leite, and J. N. Onuchic, *J. Chem. Phys.* **117**, 2172 (2002).
- ¹²V. B. P. Leite and J. N. Onuchic, *J. Phys. Chem.* **100**, 7680 (1996).
- ¹³V. B. P. Leite, *J. Chem. Phys.* **110**, 10067 (1999).
- ¹⁴V. B. P. Leite, L. C. P. Alonso, M. Newton, and J. Wang, *Phys. Rev. Lett.* **95**, 118301 (2005).
- ¹⁵H. Yang, G. B. Luo, P. Karnchanaphanurach, T. M. Louie, I. Rech, S. Cova, L. Sun, and X. S. Xie, *Science* **302**, 262 (2003); S. C. Kou and X. S. Xie, *Phys. Rev. Lett.* **93**, 180603 (2004); W. Min, G. Luo, B. J. Cherayil, S. C. Kou, and X. S. Xie, *ibid.* **94**, 198302 (2005).
- ¹⁶J. Wang and P. G. Wolynes, *Phys. Rev. Lett.* **74**, 4317 (1995); *J. Chem. Phys.* **110**, 4812 (1999).
- ¹⁷J. Wang, *J. Chem. Phys.* **118**, 952 (2003).
- ¹⁸C. L. Lee, C. T. Lin, G. Stell, and J. Wang, *Phys. Rev. E* **67**, 041905 (2003); *J. Chem. Phys.* **118**, 959 (2003).
- ¹⁹Y. Zhou, Q. Zhang, G. Stell, and J. Wang, *J. Am. Chem. Soc.* **125**, 6300 (2003).
- ²⁰J. Wang, *Biophys. J.* **87**, 2164 (2004).

- ²¹V. B. P. Leite, J. N. Onuchic, G. Stell, and J. Wang, *Biophys. J.* **87**, 3633 (2004).
- ²²B. Derrida, *Phys. Rev. Lett.* **45**, 79 (1980); *Phys. Rev. B* **24**, 2613 (1981).
- ²³J. N. Onuchic and P. G. Wolynes, *J. Phys. Chem.* **92**, 6495 (1988).
- ²⁴W. Y. Yang and M. Gruebele, *Nature (London)* **423**, 193 (2003); *Biophys. J.* **87**, 596 (2004); *J. Am. Chem. Soc.* **126**, 7758 (2004); H. Ma and M. Gruebele, *Proc. Natl. Acad. Sci. U.S.A.* **102**, 2283 (2005); *J. Comput. Chem.* **27**, 125 (2006); F. Liu and M. Gruebele, *J. Mol. Biol.* **370**, 574 (2007).